J|A|C|S ARTICLES

Published on Web 01/20/2010

Claisen Rearrangements: Insight into Solvent Effects and "on Water" Reactivity from QM/MM Simulations

Orlando Acevedo* and Kira Armacost

Department of Chemistry and Biochemistry, Auburn University, Auburn, Alabama 36849

Received October 12, 2009; E-mail: orlando.acevedo@auburn.edu

Abstract: An "on water" environment, defined by the absence of water solubility of the reactants, has been reported to provide increased rate accelerations, yields, and specificity for several types of organic reaction classes compared to organic solvents. The aromatic Claisen rearrangements of allyl *p*-R-phenyl ethers (R = CH_3, Br, and OCH_3) and allyl naphthyl ether have been investigated to determine the origin of the on water effect using QM/MM Monte Carlo calculations and free-energy perturbation theory. The simulations indicate that on water rate enhancements for the rearrangements are derived from the ability of the interfacial waters to stabilize the polar transition state via enhanced hydrogen bonding at the oil/water interface. The position and orientation of the aromatic ethers at the interface are crucial factors affecting solvent accessibility during the reaction pathway; computed solute−solvent energy pair distributions and radial distribution functions showed that hydrophobic substituents on the solute provided a more polar solvent environment than hydrophilic substituents by tilting the reacting oxygen toward the water surface. Calculations in 16 different solvents accurately reproduced the experimental trend of increased rates correlated to increasing solvent polarity. Hydrophobic effects did not provide a substantial contribution to the lowering of the free energy activation barrier (<0.5 kcal/mol), and solvent polarizability via a polarizable force field was also found to be negligible in the observed rate accelerations. New insight into solvent effects for the Claisen rearrangement is presented herein, and a QM/MM approach for computing reactions on a liquid surface is highlighted.

Introduction

Considerable attention has been directed toward the development of organic reactions that benefit from water in terms of enhanced stereoselectivities, yields, and rates; the list is extensive and reviews are available.[1−5] The interest in water as a viable alternative to organic solvents began with reports from Breslow and co-workers of significant rate accelerations for Diels−Alder reactions in aqueous solution.[6] That work and the potential advantages derived from an aqueous reaction medium in organic synthesis, e.g., safety, low cost, and ease of product isolation, has led to a widespread interest in the field. Organic cosolvents are frequently utilized to increase the solubility of organic solutes in aqueous solutions[5] and consequently much of water's unique properties, i.e., hydrophobic effect, high polarity, and high cohesive energy density, are diminished or lost.[4] However, the assumption that solubility is required for efficient catalysis has been challenged by Sharpless, who recently reported large rate and yield increases comparable to organic solvents for a variety of reactions solely "on water".[7,8] "On water" is defined as a reaction that proceeds in an aqueous organic emulsion prepared by vigorously stirring insoluble reactants with water, whereas "in water" the reactants are dissolved homogeneously in water.[7,9,10] The term "in the presence of water" has also been used interchangeably to describe on water conditions.[9] In many cases, a significant rate increase for on water reactions versus solvent-free (or "neat") reactions indicates that the rate acceleration is not simply a consequence of increased concentration of the reacting species.[1]

While the molecular details behind on water reactivity are scarce, Jung and Marcus recently proposed that free OH groups from water molecules protruding into the organic phase play a key role in catalyzing reactions via the formation of hydrogen bonds.[11] Their computational work used transition state theory (TST) and UB3LYP/6-31+G(d) energy-minimizations on the cycloaddition of quadricyclane and dimethyl azodicarboxylate complexed to three water molecules. Their interpretations have greatly enhanced the general understanding of on water catalysis. However, a major drawback associated with using a "super-

(1) Chanda, A.; Fokin, V. V. *Chem. Rev.* **2009**, *109*, 725–748.
(2) (a) Gruttadauria, M.; Giacalone, F.; Noto, R. *Adv. Synth. Catal.* **2009**, *351*, 33–57. (b) Pirrung, M. C. *Chem.—Eur. J.* **2006**, *12*, 1312–1317.
(3) (a) Shapiro, N.; Vigalok, A. *Angew. Chem., Int. Ed.* **2008**, *47*, 2849–2852. (b) Li, C.-J.; Chen, L. *Chem. Soc. Rev.* **2006**, *35*, 68–82. (c) Li, C.-J. *Chem. Rev.* **2005**, *105*, 3095–3166. (d) Li, C.-J.; Chan, T.-H. *Organic Reactions in Aqueous Media*; Wiley: New York, 1997.
(4) Lindström, U. M. *Chem. Rev.* **2002**, *102*, 2751–2772.
(5) *Organic Synthesis in Water*; Grieco, P. A., Ed.; Blackie Academic & Professional: London, 1998.
(6) (a) Rideout, D. C.; Breslow, R. *J. Am. Chem. Soc.* **1980**, *102*, 7816–7817. (b) Breslow, R. *Acc. Chem. Res.* **1991**, *24*, 159–164.
(7) Narayan, S.; Muldoon, J.; Finn, M. G.; Fokin, V. V.; Kolb, H. C.; Sharpless, K. B. *Angew. Chem., Int. Ed.* **2005**, *44*, 3275–3279.
(8) Narayan, S.; Fokin, V. V.; Sharpless, K. B. Chemistry 'on water'—Organic synthesis in aqueous suspension. In *Organic Reactions in Water*; Blackwell Publishing Ltd.: Oxford, UK, 2007; pp 350−365.
(9) Hayashi, Y. *Angew. Chem., Int. Ed.* **2006**, *45*, 8103–8104.
(10) Klijn, J. E.; Engberts, J. B. F. N. *Nature* **2005**, *435*, 746–747.
(11) (a) Jung, Y.; Marcus, R. A. *J. Am. Chem. Soc.* **2007**, *129*, 5492–5502. (b) Marcus, R. A. *J. Phys. Chem. C* **2009**, *113*, 14598–14608.

10.1021/ja908680c

Scheme 1. Claisen Rearrangement of (A) Allyl *p*-R-phenyl Ethers, R = CH_3, Br, and OCH_3, and (B) Allyl Naphthyl Ether

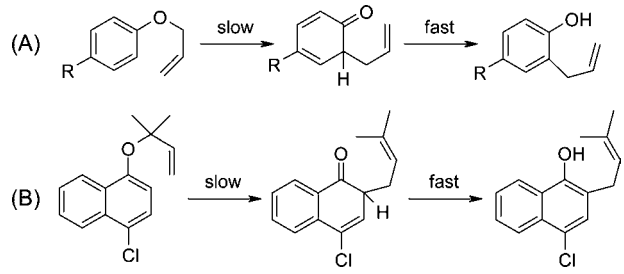

molecule complex" approach is its inability to account for hydrophobic effects. For example, the negative activation volume determined for the Claisen rearrangement of allyl vinyl ether implies that the reactant should be more destabilized relative to the activated complex in water.[12] In this work, mixed quantum and molecular mechanical (QM/MM) methodology is presented that produces a more experimentally realistic environment featuring hundreds of water molecules with the reacting organic layer lying on top.

The reaction of interest for the elucidation of on water reactivity is the Claisen rearrangement, a significant class of reactions where rate-accelerations derived from water are well-documented for aliphatic systems.[12−14] However, little is known of the effect of water on aromatic Claisen reactions (Scheme 1). Experimental rates and thermodynamic parameters have been published for the rearrangement of allyl *p*-tolyl ether (R = CH_3 in Scheme 1A) in the gas phase and in 17 solvents of different polarities.[15] The solvent dependence of rates for Claisen reactions is complex and does not show simple increases with increasing solvent polarity. In fact, the rates in phenol and water are about the same and 300 times greater than in vacuum for the ether rearrangement.[15] A detailed understanding of its origin is currently unclear except that it is primarily a transition state effect.[15,16]

QM/MM calculations featuring the PDDG/PM3 semiempirical QM method coupled to free energy perturbation (FEP) theory and Monte Carlo (MC) simulations have been carried out for the four Claisen rearrangements shown in Scheme 1 on water, in water, and in 14 additional solvents, viz. *p*-chlorophenol, phenol, *p*-cresol, ethylene glycol, 2-aminoethanol, diethylene glycol monoethyl ether (carbitol), sulfolane, adiponitrile, propylene carbonate, *n*-decylamine, methanol, acetonitrile, DMF, and toluene. Activation barriers, solute−solvent interaction energies, and radial distribution functions have been computed with complete sampling of the solute to elucidate the role of solvation on the reactants and activated complexes. Substituent effects were investigated using R = CH_3, Br, and OCH_3 groups in allyl *p*-R-phenyl ethers (Scheme 1A).[17] The aromatic Claisen rearrangement of allyl naphthyl ether (Scheme 1B), reported by Sharpless and co-workers to provide better yields and rates on water when compared to typical organic solvents,[7] was also computed in this investigation. In addition, a detailed comparison of alternative methods to our QM/MM approach is given. Notably, high-level ab initio and density functional theory (DFT) calculations at the CBS-QB3 and B3LYP theory levels, respectively, coupled to a continuum solvent model failed to predict the sequence of reaction rates in solution.

New insight into on water Claisen rearrangement reactions is presented herein, and a novel QM/MM approach for accurately predicting solvent-promoted rate accelerations at the air/water interface is highlighted. In addition, solvent effects on aromatic Claisen rearrangements from different classes of solvent, e.g., protic, polar aprotic, and nonpolar, are discussed in detail and changes along the reaction pathway are fully characterized. To our knowledge, this work is the first QM/MM study of a reaction on a liquid surface featuring hundreds of solvent molecules. Reported benefits of an on water aqueous medium for multiple reaction types open up many additional systems for study and interpretation using the present QM/MM methodology, e.g., cycloadditions, Diels−Alder, and epoxide opening reactions.[1,2,7]

Computational Methods

Reactants and transition states were located in hundreds of explicit solvent molecules represented using the TIP4P water model[18] and the OPLS-AA force field for nonaqueous solutions.[19,20] The solutes were treated using the PDDG/PM3 semiempirical QM method,[21] which has given excellent results for a wide variety of organic and enzymatic reactions in the solution phase.[22−26] Computation of the QM energy and atomic charges is performed for each attempted move of the solute, which occurs every 100 configurations. For electrostatic contributions to the solute−solvent energy, CM3 charges[27] were obtained for the solute with a scaling factor of 1.14. Lennard-Jones interactions between solutes and solvent atoms were taken into account using OPLS parameters. This combination is appropriate for a PM3-based method, as it minimizes errors in the computed free energies of hydration.[28] Changes in free energy were calculated using free energy perturbation (FEP) theory in conjunction with NPT Metropolis Monte Carlo (MC)

(12) Gajewski, J. J. *Acc. Chem. Res.* **1997**, *30*, 219–225.
(13) (a) Majumdar, K. C.; Alam, S.; Chattopadhyay, B. *Tetrahedron* **2008**, *64*, 597–643. (b) Gao, J. *J. Am. Chem. Soc.* **1994**, *116*, 1563–1564. (c) Severance, D. L.; Jorgensen, W. L. *J. Am. Chem. Soc.* **1992**, *114*, 10966–10968.
(14) Cramer, C. J.; Truhlar, D. G. *J. Am. Chem. Soc.* **1992**, *114*, 8794–8799.
(15) White, W. N.; Wolfarth, E. F. *J. Org. Chem.* **1970**, *35*, 2196–2199.
(16) White, W.; Slater, C.; Fife, W. *J. Org. Chem.* **1961**, *26*, 627–628.
(17) White, W. N.; Wolfarth, E. F. *J. Org. Chem.* **1970**, *35*, 3585.
(18) Jorgensen, W. L.; Chandrasekhar, J.; Madura, J. D.; Impey, W.; Klein, M. L. *J. Chem. Phys.* **1983**, *79*, 926–935.
(19) Jorgensen, W. L.; Maxwell, D. S.; Tirado-Rives, J. *J. Am. Chem. Soc.* **1996**, *118*, 11225–11236.
(20) Jorgensen, W. L.; Tirado-Rives, J. *Proc. Natl. Acad. Sci. U.S.A.* **2005**, *102*, 6665–6670.
(21) (a) Tubert-Brohman, I.; Guimarães, C. R. W.; Jorgensen, W. L. *J. Chem. Theory Comput.* **2005**, *1*, 817–823. (b) Tubert-Brohman, I.; Guimarães, C. R. W.; Repasky, M. P.; Jorgensen, W. L. *J. Comput. Chem.* **2003**, *25*, 138–150. (c) Repasky, M. P.; Chandrasekhar, J.; Jorgensen, W. L. *J. Comput. Chem.* **2002**, *23*, 1601–1622.
(22) Acevedo, O.; Jorgensen, W. L. *Acc. Chem. Res.* **2010**, *43*, 142−151.
(23) Sheppard, A. N.; Acevedo, O. *J. Am. Chem. Soc.* **2009**, *131*, 2530–2540.
(24) Sambasivarao, S. V.; Acevedo, O. *J. Chem. Theory Comput.* **2009**, *5*, 1038–1050.
(25) (a) Acevedo, O.; Squillacote, M. E. *J. Org. Chem.* **2008**, *73*, 912–922. (b) Acevedo, O.; Jorgensen, W. L. *J. Am. Chem. Soc.* **2006**, *128*, 6141–6146. (c) Acevedo, O.; Jorgensen, W. L. *J. Org. Chem.* **2006**, *71*, 4896–4902. (d) Acevedo, O.; Jorgensen, W. L. Solvent effects on organic reactions from QM/MM simulations. In *Annual Reports in Computational Chemistry*; Spellmeyer, D., Ed.; Elsevier: New York, 2006; Vol. 2, pp 263−278; (e) Tubert-Brohman, I.; Acevedo, O.; Jorgensen, W. L. *J. Am. Chem. Soc.* **2006**, *128*, 16904–16913. (f) Acevedo, O.; Jorgensen, W. L. *J. Am. Chem. Soc.* **2005**, *127*, 8829–8834. (g) Acevedo, O.; Jorgensen, W. L. *Org. Lett.* **2004**, *6*, 2881–2884.
(26) (a) Acevedo, O.; Jorgensen, W. L. *J. Chem. Theory Comput.* **2007**, *3*, 1412–1419. (b) Acevedo, O.; Jorgensen, W. L.; Evanseck, J. D. *J. Chem. Theory. Comput.* **2007**, *3*, 132–138.
(27) Thompson, J. D.; Cramer, C. J.; Truhlar, D. G. *J. Comput. Chem.* **2003**, *24*, 1291–1304.
(28) Blagović, M. U.; Morales de Tirado, P.; Pearlman, S. A.; Jorgensen, W. L. *J. Comput. Chem.* **2004**, *25*, 1322–1332.

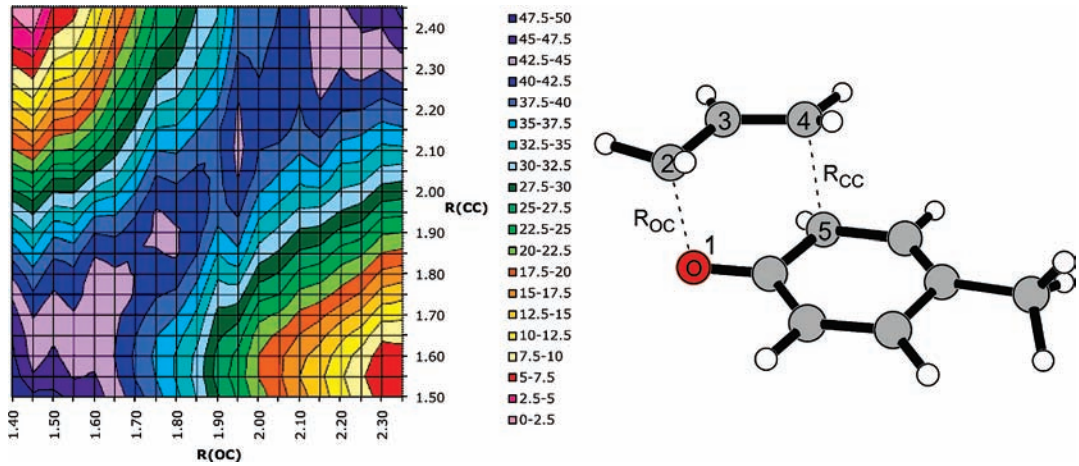

Figure 1. Free energy map (kcal/mol) computed for the on water Claisen rearrangement of allyl *p*-tolyl ether using the reaction coordinates R_{OC} and R_{CC}. The illustrated structure is the transition structure from the QM/MM/MC simulations.

simulations at 25 °C and 1 atm. Each FEP calculation entailed ca. 40 million configurations of equilibration and 20 million configurations of averaging using increments of 0.01 Å for the making/breaking bond distances (Figure 1).

To explore the effect of various solvents upon the Claisen rearrangement, new OPLS-AA solvent boxes were constructed in a fashion similar to previous work.[24] Briefly, the liquid-phase simulations were carried out by placing 400 solvent molecules at random positions in the simulation box. The boxes were then equilibrated at 25 °C for 100−400 million MC steps in the NPT ensemble. In the case of long-chain molecules, e.g., carbitol and *n*-decylamine, an initial temperature value of 1000 °C was applied prior to equilibration for 10 million configurations in the NVT ensemble to encourage a thorough mixing. The initial heating has been shown to provide improved convergence of MC simulations for long-chain alkanes and ionic liquids.[24,29] The computed liquid densities and heats of vaporization (ΔH_{vap}) for the solvent boxes were found to be in good agreement with experiment. A complete table comparing the computed and experimental densities and ΔH_{vap} is given in the Supporting Information as Table S1, and OPLS atom types for all solvents simulated are given in Figure S1.

BOSS was used to carry out all QM/MM reactions from the stored and custom-made solvent boxes.[30] All solvents were fully flexible, i.e., all bond stretching, angle bending, and torsional motions were sampled, with the exception of water, acetonitrile,[31] and methanol,[32] which already exist in BOSS as fixed united-atom solvents. Periodic boundary conditions have been applied to tetragonal boxes containing between 400 and 750 solvent molecules. Solute−solvent and solvent−solvent cutoffs of 10−12 Å were employed with quadratic feathering of the intermolecular interactions within 0.5 Å of the cutoff. Adjustments to the allowed ranges for rotations, translations, and dihedral angle movements led to overall acceptance rates of 30−50% for new configurations. The ranges for bond stretching and angle bending were set automatically by the BOSS program on the basis of force constants and temperature. All QM/MM/MC calculations were run on a Linux cluster at Auburn University.

The complete basis set method CBS-QB3[33] was also used to characterize the transition structures and ground states in vacuum using Gaussian 09.[34] In a recent study, the CBS-QB3 method gave energetic results in the closest agreement to experiment for a set of 11 different pericyclic reactions compared to other ab initio and density functional theory (DFT) methods.[35] The CBS-QB3 calculations were used for geometry optimizations and computations of vibrational frequencies, which confirmed all stationary points as either minima or transition structures and provided thermodynamic corrections. The effect of solvent was approximated by subsequent optimization and vibrational frequency calculations using the polarizable continuum model (PCM)[36] and the B3LYP/6-311+G(2d,p) theory level.[37] All ab initio calculations were performed on computers located at the Alabama Supercomputer Center.

Results and Discussion

Structures. Configurationally averaged free-energy maps, ΔG (kcal/mol), were computed for the aromatic Claisen rearrangements (Scheme 1) in 16 different solvents by perturbing the reacting bond distances R_{OC} and R_{CC} via potentials of mean force (PMF) calculations in increments of 0.05 Å (Figure 1). To locate the critical points more precisely, the regions surrounding the free-energy minima and maxima from the initial maps were explored using increments of 0.01 Å. This provided refined results for the geometries and activation barriers, as summarized in Tables 1−4 and Supporting Information Tables S2−S4. All internal degrees of freedom, minus the R_{OC} and R_{CC} reaction coordinates, were fully sampled during the simulations. It was necessary to use multiple gas-phase optimized structures to provide good starting points for the reaction profile. Each solution-phase free energy perturbation (FEP) calculation required approximately 120 million single point QM calculations per free-energy map, illustrating the need for highly efficient QM methods.

The on water reactions were carried in out in a similar fashion to the homogeneous solution-phase calculations, except that periodicity was removed from the *z*-axis of an explicit 500 water molecule box and the ether was placed on top of the *z*-axis; an

(29) Thomas, L. L.; Christakis, T. J.; Jorgensen, W. L. *J. Chem. Phys. B* **2006**, *110*, 21198–21204.
(30) Jorgensen, W. L.; Tirado-Rives, J. *J. Comput. Chem.* **2005**, *26*, 1689–1700.
(31) Jorgensen, W. L.; Briggs, J. M. *Mol. Phys.* **1988**, *63*, 547–558.
(32) Jorgensen, W. L. *J. Phys. Chem.* **1986**, *90*, 1276–1284.
(33) Ochterski, J. W.; Petersson, G. A.; Montgomery, J. A. *J. Chem. Phys.* **1996**, *104*, 2598–2619.
(34) Frisch, M. J.; et al. Gaussian 09, Revision A.1; Gaussian: Wallingford, CT, 2009 (Full reference given in the Supporting Information).
(35) Guner, V.; Khuong, K. S.; Leach, A. G.; Lee, P. S.; Bartberger, M. D.; Houk, K. N. *J. Phys. Chem. A* **2003**, *107*, 11445–11459.
(36) Tomasi, J.; Mennucci, B.; Cammi, R. *Chem. Rev.* **2005**, *105*, 2999–3093.
(37) (a) Becke, A. D. *J. Chem. Phys.* **1993**, *98*, 5648–5652. (b) Lee, C.; Yang, W.; Parr, R. G. *Phys. Rev.* **1988**, *37*, 785–789.

Table 1. Computed Bond Lengths (Å) for the Allyl *p*-Tolyl Ether Claisen Rearrangement Transition Structures at 25 °C and 1 atm

	R_{OC}	R_{CC}
p-chlorophenol	1.88	2.00
in water	1.87	2.01
phenol	1.87	2.00
p-cresol	1.84	1.97
ethylene glycol	1.86	1.97
on water	1.86	1.97
2-aminoethanol	1.84	1.98
carbitol	1.86	1.98
sulfolane	1.86	1.97
adiponitrile	1.87	1.97
propylene carbonate	1.86	1.99
n-decylamine	1.83	1.97

[a] From the 2D free-energy maps computed in the QM/MM/MC/FEP simulations.

Table 2. Absolute Free Energy of Activation, $\Delta G^{\ddagger}$ (kcal/mol), at 25 °C for the Claisen Rearrangement of Allyl *p*-Tolyl Ether and the $\Delta\Delta G^{\ddagger}$ Relative to in Water using QM/MM

	$\Delta G^{\ddagger}$		$\Delta\Delta G^{\ddagger}$	
	calcd[a]	exptl[b]	calcd[a]	exptl[b]
p-chlorophenol	47.9	33.4	–0.8	–1.0
in water	48.8	34.4[c]	0.0	0.0[c]
phenol	49.1	34.4	0.4	0.0
p-cresol	48.7	34.7	0.0	0.3
ethylene glycol	48.7	34.7	0.0	0.3
on water	49.6	–	0.9	–
2-aminoethanol	49.7	35.5	1.0	1.1
carbitol	50.0	35.9	1.3	1.5
sulfolane	50.5	36.3	1.8	1.9
adiponitrile	50.7	36.4	2.0	2.0
propylene carbonate	50.8	36.5	2.1	2.1
n-decylamine	51.4	37.1	2.7	2.7

[a] PDDG/PM3 and MC/FEP. [b] From ref 15 at 170 °C; experimental error for $\Delta G^{\ddagger}$ is ca. ± 0.3 kcal/mol. [c] 28.5% EtOH–H_2O.

Table 3. Absolute Free Energy of Activation, $\Delta G^{\ddagger}$ (kcal/mol), at 25 °C for the Claisen Rearrangement of Allyl *p*-R-phenyl Ethers and the $\Delta\Delta G^{\ddagger}$ Relative to $R = CH_3$ Using QM/MM Simulations

	$\Delta G^{\ddagger}$		$\Delta\Delta G^{\ddagger}$	
R	calcd[a]	exptl[b]	calcd[a]	exptl[b]
		In Water		
OCH_3	47.6	33.5	–1.1	–0.9
CH_3	48.8	34.4	0.0	0.0
Br	49.1	34.9	0.4	0.5
		On Water		
OCH_3	48.5	–	–1.1	–
CH_3	49.6	–	0.0	–
Br	50.1	–	0.5	–

[a] PDDG/PM3/MC/FEP. [b] Experimental values for 28.5% EtOH–H_2O at 170 °C (ref17).

equilibrated NVT water slab was used to prevent a very slow drift of the water molecules that reduces the exposed surface, i.e., stretch in the *z*-direction. An orientation analysis of multiple snapshots of allyl *p*-tolyl ether relative to the surface of the slab (perpendicular to the *z*-axis) found that the aromatic ring tended to lie essentially flat on the surface with a slight tilt toward the oxygen, while the allyl side chain occupied the gas-phase (Figures 2 and S2, Supporting Information). Hydrogen bonding was found to be primarily responsible for the orientation, i.e., favorable interactions between water and the π-system of the aromatic ring and the oxygen. A similar orientation was found for allyl naphthyl ether, where the fused aromatic rings lay essentially flat on the surface of the water slab with a tilt toward

Table 4. Computed Free Energy of Activation, $\Delta G^{\ddagger}$ (kcal/mol), at 25 °C for the Claisen Rearrangement of Allyl Naphthyl Ether and the $\Delta\Delta G^{\ddagger}$ Relative to in Water

	QM/MM[a]		PCM[b]	
	$\Delta G^{\ddagger}$	$\Delta\Delta G^{\ddagger}$	$\Delta G^{\ddagger}$	$\Delta\Delta G^{\ddagger}$
in water	40.7	0.0	20.0	0.0
on water	41.3	0.6	–	–
CH_3CN	41.1[c]	0.4	20.1	0.1
MeOH	43.5	2.8	20.1	0.1
DMF	43.9	3.2	20.1	0.1
toluene	42.5	1.8	21.8	1.8

[a] PDDG/PM3/MC/FEP. [b] Optimized using B3LYP/6-311+G(2d,p). [c] Using a united-atom OPLS solvent model. The all-atom version gave a $\Delta G^{\ddagger}$ of 40.8 kcal/mol.

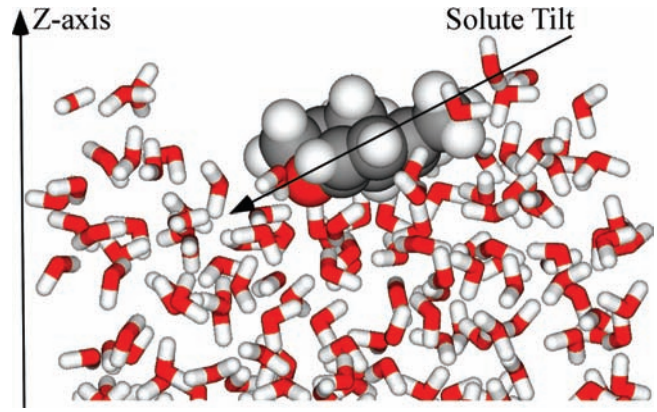

Figure 2. Illustration of the on water allyl *p*-tolyl ether transition structure from the QM/MM/MC Claisen rearrangement calculations.

the oxygen atom (Supporting Information Figure S3). The addition of hydrophilic substituents on the phenyl ring, e.g., R = OCH_3 in the allyl *p*-R-phenyl ethers, strongly tilted the ring on the surface toward the substituent and as a result tilted the reacting oxygen away from the interfacial waters, reducing the number of hydrogen bonds available (see "Radial Distributions Functions").

The calculations showed that, although solvent effects can produce a rate acceleration of up to 100-fold,[15] the transition structure geometries do not show large variations among different solvents, e.g., R_{OC} of 1.86 ± 0.02 Å and R_{CC} of 1.98 ± 0.02 Å for the allyl *p*-tolyl ether reactions (Table 2). Secondary deuterium kinetic isotope effect (KIE) experiments on related allyl vinyl (and phenyl) ethers also found the transition state to be solvent-insensitive with no significant bond breaking increase in aqueous media compared to nonpolar solvents.[12,38] CBS-QB3 calculations predicted an earlier activated complex for allyl *p*-tolyl ether with gas-phase R_{OC} and R_{CC} distances of 2.16 and 2.25 Å, respectively; B3LYP/6-311+G(2d,p) gave similar results, i.e., 2.17 and 2.25 Å. The trend of earlier transition structures for the ab initio and DFT calculations compared to PDDG/PM3 was also found in the other Claisen rearrangements studied (see Supporting Information Tables S2−S4 for gas- and solution-phase geometries of the allyl *p*-R-phenyl ethers and allyl naphthyl ether). All theory levels used were consistent with KIE measurements which indicated that the activated complex should resemble the reactant with more C−O bond cleavage than C−C bond formation occurring.[12] In the case of allyl naphthyl ether, the R_{OC} and R_{CC} distances at

(38) Gajewski, J. J.; Brichford, N. L. *J. Am. Chem. Soc.* **1994**, *116*, 3165–3166.

the transition state were found to slightly increase with increasing solvent polarity, e.g., 1.83, 1.84, 1.86, 1.87, 1.89, and 1.90 Å for toluene, DMF, acetonitrile, methanol, in water, and on water, respectively, for the R_{OC} distance (Table S4, Supporting Information).

Energetics. The absolute $\Delta G^{\ddagger}$ values at 25 °C computed from the QM/MM/MC simulations were overestimated by an average of ca. 14 kcal/mol compared to experiment at 170 °C; however, excellent computed $\Delta\Delta G^{\ddagger}$ (kcal/mol) values between different solvents were found (Table 2). Error ranges in the computed free-energy values have been estimated from fluctuations in the ΔG values for each FEP window using the batch means procedure with batch sizes of 0.5 million configurations; calculated errors in the free energies imply overall uncertainties in the $\Delta G^{\ddagger}$ of ca. 0.4 kcal/mol. The $\Delta G^{\ddagger}$ overestimation is a systematic error common in pericyclic reactions when employing a semiempirical method.[39] Similar errors have been reported for the Claisen rearrangement of chorismate to prephenate using the AM1 method.[40] Cramer and Truhlar also reported an underestimation of the absolute rate accelerations for aqueous allyl vinyl ether and derivative Claisen rearrangements when employing AM1.[14] The authors concluded that a systematic underestimation of the charges at the transition states was responsible, but the analogous trends in charge reported from the AM1-SM1 model provided excellent relative solvation free energies for the reacting species.[14,41] It is important to note that the overestimation of the absolute $\Delta G^{\ddagger}$ value using semiempirical QM/MM methods is not limited to the Claisen rearrangement, as similar findings have been reported for multiple Diels−Alder reactions,[26,42] ene reactions,[23] and methyl transfer reactions.[43]

Potentially, a simple reparameterization of the PDDG/PM3 Hamiltonian by scaling the energies from points along the reaction coordinate could provide accurate $\Delta G^{\ddagger}$ values; however, the physical reasons for determining structures would be absolutely the same as the original Hamiltonian. Hence, there is no difference in leaving the Hamiltonian in its original form or in scaling the energies when one considers the relative energies computed. The close $\Delta\Delta G^{\ddagger}$ agreement indicates that solvent effects on the Claisen rearrangements are being appropriately modeled (Table 2). Notably, recent B3LYP/6-31G(d) calculations using the polarizable continuum model (PCM) failed to predict the accurate sequence of reaction rates for the allyl *p*-tolyl ether rearrangement in solution.[44] Higher theory levels coupled to improved PCM models gave similar results in this work (see Table 4 and the "Continuum Solvent Model"). An additional approach for the improvement of the $\Delta G^{\ddagger}$ values is the assignment of specific Lennard-Jones terms for every atom type in the Claisen rearrangements as opposed to the general OPLS empirical parameters chosen for each atom in the QM region, e.g., C, O, H. Optimization of the Lennard-Jones parameters embedded in the hydrid QM/MM potential, as pioneered by Gao, has been successful for multiple organic reaction studies.[45] However, preliminary testing found the results to be nearly identical to the present methodology.

Of particular interest is that the $\Delta\Delta G^{\ddagger}$ for the on water reaction was predicted to be only ca. 0.9 and 0.6 kcal/mol higher in energy than the same reaction homogeneously dissolved in pure aqueous solution for the allyl *p*-R-phenyl ethers and allyl naphthyl ether, respectively (Tables 2−4). This prediction places the rate of reaction for the on water environment in-line with that of polar aprotic solvents and potentially faster than half of the solvents tested. The results are consistent with experimental observations by Sharpless on the allyl naphthyl ether Claisen rearrangement and with other recent work on cycloaddition and Wittig reactions.[7,8,46]

Solvent Effects on the Rate of Reaction. In the Claisen rearrangement study of allyl *p*-tolyl ether by White and Wolfarth, the rate of reaction was found to increase with increasing solvent polarity as defined using a *Z* factor[47] correlation at 25 °C.[15] However, no specific characteristic of the solvent polarity could be attributed to the rate accelerations. For example, while hydrogen bonding may play a large role and the fastest rates generally occurred in hydroxylic solvents, the reaction was also equally as fast in some nonhydroxylic solvents, e.g., propylene carbonate compared to 2-octanol. In addition, while increased solvent acidity also appeared to increase rates, no clear correlation exists, e.g., the reaction was a factor of 2.8 slower in octanoic acid as compared to *p*-chlorophenol.[15] The major difficulty associated with determining the origin of the solvent effects on the rate of the Claisen rearrangement is that solvent polarity can be a composite of many different properties, including solvent polarizability, hydrogen-bonding ability, and dipole moment. Resolving their individual contributions on the reaction is extremely difficult from an experimental perspective. However, detailed insight on the changes in solvation along the reaction pathway is available from the present QM/MM/MC calculations. The relationship between the structures, solvent properties, rates, and energies is discussed below.

Solvent Polarization. Fixed charges on the solvent molecules, derived from the OPLS-AA force field,[19] were used to model the electrostatic interactions occurring between the solvent and solute in the QM/MM simulations; this approach utilizing nonpolarizable potential functions for the solvent molecules has been successful in accurately reproducing condensed-phase effects on a large variety of organic reactions.[22] However, solvent polarizability is often cited as a necessary criterion for accurately reproducing solvent effects, particularly for low dielectric systems.[48,49] To test the effect of solvent polarization upon the Claisen rearrangement, calculation of the allyl *p*-tolyl ether reaction in polarizable phenol was carried out. An approach identical to that reported in a recent paper by Jorgensen et al. was employed, in which inducible dipoles were added to nonhydrogen atoms and nonbonded interactions were handled using

(39) Sattelmeyer, K. W.; Tubert-Brohman, I.; Jorgensen, W. L. *J. Chem. Theory Comput.* **2006**, *2*, 413–419.
(40) Repasky, M. P.; Guimarães, C. R. W.; Chandrasekhar, J.; Tirado-Rives, J.; Jorgensen, W. L. *J. Am. Chem. Soc.* **2002**, *125*, 6663–6672.
(41) Cramer, C. J.; Truhlar, D. G. *Science* **1992**, *256*, 213–217.
(42) Chandrasekhar, J.; Shariffskul, S.; Jorgensen, W. L. *J. Phys. Chem. B* **2002**, *106*, 8078–8085.
(43) Gunaydin, H.; Acevedo, O.; Jorgensen, W. L.; Houk, K. N. *J. Chem. Theory Comput.* **2007**, *3*, 1028–1035.
(44) Irani, M.; Haqgu, M.; Talebi, A.; Gholami, M. R. *J. Mol. Struct. (THEOCHEM)* **2009**, *893*, 73–76.
(45) Gao, J. *Acc. Chem. Res.* **1996**, *29*, 298–305.
(46) (a) Butler, R. N.; Coyne, A. G.; Cunningham, W. J.; Moloney, E. M.; Burke, L. A. *Helv. Chim. Acta* **2005**, *88*, 1611–1629. (b) Dambacher, J.; Zhao, W.; El-Batta, A.; Anness, R.; Jiang, C.; Bergdahl, M. *Tetrahedron Lett.* **2005**, *46*, 4473–4477.
(47) Kosower, E. M. *J. Am. Chem. Soc.* **1958**, *80*, 3253–3260.
(48) (a) Jorgensen, W. L.; McDonald, N. A.; Selmi, M.; Rablen, P. R. *J. Am. Chem. Soc.* **1995**, *117*, 11809–11810. (b) Wick, C. D.; Kuo, I.-F. W.; Mundy, C. J.; Dang, L. X. *J. Chem. Theory Comput.* **2007**, *3*, 2002–2010. (c) Marenich, A. V.; Olson, R. M.; Chamberlin, A. C.; Cramer, C. J.; Truhlar, D. G. *J. Chem. Theory Comput.* **2007**, *3*, 2055–2067.
(49) Jorgensen, W. L.; Jensen, K. P.; Alexandrova, A. N. *J. Chem. Theory Comput.* **2007**, *3*, 1987–1992.

a OPLS/CM1A approach; improved interaction energies were reported for anion−phenol complexes when using this polarizable model.[49] The electric field that determines the inducible dipoles is computed from the permanent charges using eq 1, and the polarization energy is given by eq 2. The same first-order polarization model has been used in earlier studies with good success.[50] Values of 1.0 and 1.5 Å^3 for the polarizabilities, α_i, on carbon and heteroatoms, respectively, were used.[49] The $\Delta G^{\ddagger}$ values computed for the allyl *p*-tolyl ether reaction using the polarized OPLS/CM1A versus unpolarized OPLS-AA solvent models were 49.2 and 49.1 kcal/mol, respectively. The transition structure geometries were also essentially identical with R_{OC} and R_{CC} distances of 1.87 and 2.00 Å compared to 1.87 and 1.99 Å in the polarized and unpolarized phenol. Solvent polarization was not found to provide an essential contribution in the observed rate accelerations for the Claisen rearrangement, at least when considering phenol, which should be a good candidate for polarization effects in view of its low dielectric constant ($\varepsilon = 9.9$).

$$\vec{\mu}_i = \alpha_i \vec{E}_i^0 \tag{1}$$

$$E_{pol} = -\frac{1}{2}\sum_i \vec{\mu}_i \vec{E}_i^0 \tag{2}$$

Substituent Effects on Energetics. Substituent effects on the Claisen rearrangement were studied with the inclusion of R = OCH_3, CH_3, and Br groups in the allyl *p*-R-phenyl ethers. The computed energies in water and on water were in good agreement with experimental free energies of activation relative to CH_3 (Table 3), e.g., computed $\Delta\Delta G^{\ddagger}$ values of 0.4, 0.0, and −1.1 kcal/mol compared to experimental values of 0.5, 0.0, and −0.9 kcal/mol for the Br, CH_3, and OCH_3 reactions in water, respectively. Correlation of experimental rate constants for *p*-substituted allyl phenyl ethers with different substituents has shown that electron-donating groups weaken the reacting carbon−oxygen bond and increase the rate for both thermal- and photo-Claisen rearrangements.[51] However, R = Br in allyl *p*-R-phenyl ether has a reduced reaction rate compared to OCH_3 and CH_3. Bond dissociation energy (BDE) in phenol has been shown to be strongly dependent on substituents; experimental measurements and theoretical work indicate that halogen substituents have only a minor effect on the BDE for cleavage reactions of phenolic ethers as compared to methoxy substituents.[52] This may originate from the strong electron-withdrawing inductive effect of Br outweighing its weak electron-donating resonance effect. However, the current aqueous phase simulations also suggest that site-specific hydrogen bonding between the reacting oxygen of the ether and the water molecules and accessibility of the interfacial waters to the solute play a large role on the rate accelerations (see "Radial Distribution Functions").

Allyl naphthyl ether was also computed in water, on water, and in four additional solvents, i.e., methanol, acetonitrile, DMF, and toluene (Table 4). Activation barriers have not been reported experimentally; however, a qualitative representation of the rates and yields were given by Sharpless and co-workers.[7] The on water environment for the allyl naphthyl ether rearrangement was observed to produce faster rates at 23 °C (5 days for complete reaction to occur) compared to neat conditions (6 days) and organic solvents (>6 days). A 100% yield was reported for the on water reaction and provided the best set of conditions despite the modest rate acceleration.[7] The current calculations are consistent with the experimental results predicting on water to have a faster rate than all other solvents computed with the exception of acetonitrile and the in water reactions. Acetonitrile used a three-site united-atom model[31] which could potentially have affected the results, as most reactions computed used an all-atom OPLS model.[19] Accordingly, an all-atom acetonitrile solvent box was constructed in an identical fashion to the other solvents and used to recompute the Claisen rearrangement of allyl naphthyl ether. The $\Delta G^{\ddagger}$ was not dramatically changed as the predicted activation barrier fell within the computed error range of ±0.4 kcal/mol ($\Delta G^{\ddagger}$ = 40.8 and 41.1 kcal/mol in the all-atom and united-atom CH_3CN models, respectively).

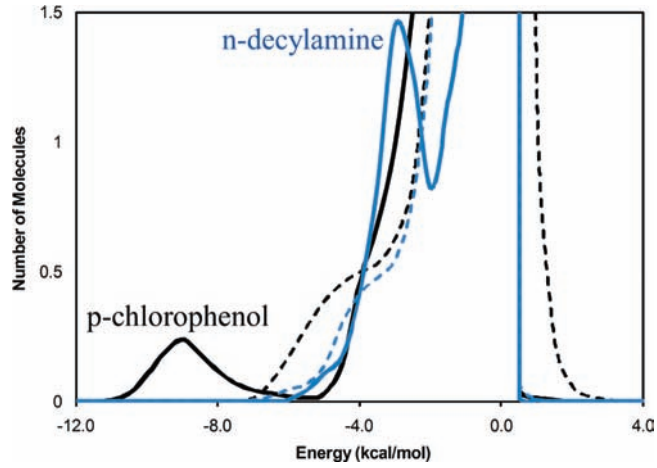

Figure 3. Solute−solvent energy pair distributions for the Claisen rearrangement of allyl *p*-tolyl ether in *p*-chlorophenol, transition structure (solid black) and reactant (dashed black), and in n-decylamine, transition structure (solid blue) and reactant (dashed blue), at 25 °C. The ordinate records the number of solvent molecules that interact with the solutes and their interaction energy is on the abscissa.

Solute−Solvent Energy Pair Distributions. To elucidate the fact that reaction rates increase with increasing solvent polarity (as defined by *Z* values),[15] solute−solvent energy pair distributions were computed for all reactions studied. Solute−solvent energy pair distributions record the average number of solvent molecules that interact with the solute and their associated energy. The interaction energies are quantified by analyzing the QM/MM/MC results near the reactant and at the transition structure FEP windows. The results for the Claisen rearrangement of allyl *p*-tolyl ether in *p*-chlorophenol and *n*-decylamine are shown in Figure 3, results for the allyl *p*-R-phenyl ethers in water and on water are given in Figure 4, and the values for all other solvents and allyl naphthyl ether are found in Figures S4−S6 of the Supporting Information. Hydrogen bonding in water and on water and the most favorable electrostatic interactions in the nonaqueous solvents are reflected in the left-most region, with solute−solvent interaction energies more attractive than −4 kcal/mol. The large bands near 0 kcal/mol result from the many distant solvent molecules in the outer shells.

(50) (a) Gao, J. *J. Comput. Chem.* **1997**, *18*, 1061–1071. (b) Straatsma, T. P.; McCammon, J. A. *Chem. Phys. Lett.* **1991**, *177*, 433–440. (c) King, G.; Warshel, A. *J. Chem. Phys.* **1990**, *93*, 8682–8692.
(51) (a) White, W. N.; Gwynn, D.; Schlitt, R.; Girard, C.; Fife, W. *J. Am. Chem. Soc.* **1958**, *80*, 3271–3277. (b) Goering, H. L.; Jacobson, R. R. *J. Am. Chem. Soc.* **1958**, *80*, 3277–3285. (c) Pincock, A. L.; Pincock, J. A.; Stefanova, R. *J. Am. Chem. Soc.* **2002**, *124*, 9768–9778.
(52) (a) Mulder, P.; Saastad, O. W.; Griller, D. *J. Am. Chem. Soc.* **1988**, *110*, 4090–4092. (b) Pratt, D. A.; Wright, J. S.; Ingold, K. U. *J. Am. Chem. Soc.* **1999**, *121*, 4877–4882.

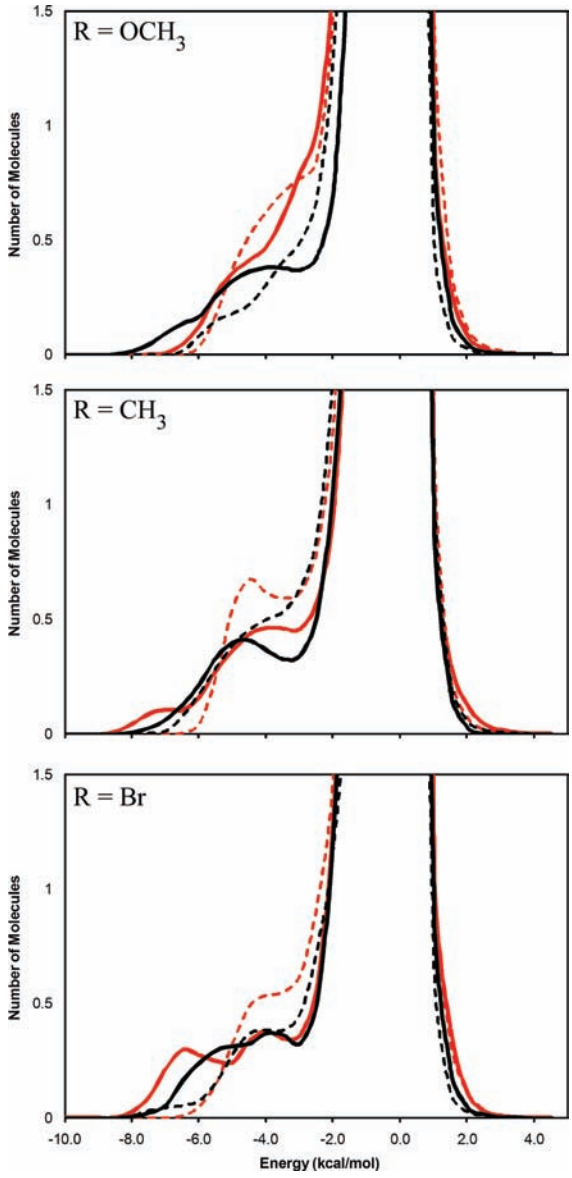

Figure 4. Solute−solvent energy pair distributions for the Claisen rearrangement of allyl *p*-R-phenyl ethers: in water transition structure (solid red), in water reactant (dashed red), on water transition structure (solid black), and on water reactant (dashed black) at 25 °C.

It is immediately clear in viewing Figure 3 that there is a much greater gain in very favorable solute−solvent interactions when proceeding from the reactant to the transition structure in the most polar nonaqueous solvent studied, *p*-chlorophenol, compared to the least polar, *n*-decylamine. The low-energy band in *p*-chlorophenol arises from favorable electrostatic interactions with the more dipolar transition structure, i.e., hydrogen bonding between the hydroxyl group of the solvent and the oxygen of the ether, and favorable $\pi-\pi$ stacking between the aromatic rings; these interactions diminish dramatically in *n*-decylamine. Integration of the transition structure band from −12 to −5.5 kcal/mol yields 1.1 *p*-chlorophenol molecules and 0.5 *n*-decylamine molecules (expanding the integration to −4 kcal/mol increases the number of *n*-decylamine molecules to 0.7). The average strength of the peak for *p*-chlorophenol at the transition structure is at −9 kcal/mol, which weakens to −3 kcal/mol for *n*-decylamine. The results are consistent with experimental findings that transition state effects are primarily

Table 5. Solute−Solvent Energy Pair Distributions for the Claisen Rearrangement of Allyl *p*-R-phenyl Ethers and Allyl Naphthyl Ether for the Reactant (GS) and Transition Structure (TS) in Water and on Water Integrated to −4.0 kcal/mol (−3.5 kcal/mol in parentheses)[a]

	in water		on water	
R	GS	TS	GS	TS
OCH_3	1.7 (2.5)	1.7 (2.3)	1.0 (1.4)	1.8 (2.2)
CH_3	2.2 (2.7)	2.1 (2.5)	1.9 (2.4)	2.0 (2.3)
Br	1.6 (2.1)	2.1 (2.5)	1.4 (1.8)	1.8 (2.2)
naphthyl	2.0 (2.6)	2.6 (3.1)	1.1 (1.5)	2.0 (2.4)

[a] From Figures 4 and S6 (Supporting Information).

responsible for rate accelerations (determined by alkyl and aryl substitutions at the α- and γ-positions in the allyl side chain).[16] Inspection of the solute−solvent energy pair distributions for the other eight nonaqueous solvents finds a general trend of weaker and less specific dipole−dipole interactions between the solvent and the allyl *p*-tolyl ether transition structure as the solvent polarity diminishes (Figures S4 and S5, Supporting Information).

Of more relevance to the on water reactivity is the exact nature of the favorable solute−solvent interactions in the aqueous environments relative to the conventional organic solvents. Comparison of the in water and on water systems also found stronger bands at the activated complex, shown as solid red and black lines in Figure 4, relative to the reactants (dashed lines). Integration of these bands from −12 to −4 kcal/mol results in 2.2 and 2.1 water molecules interacting with the allyl *p*-tolyl ether reactant and transition state, respectively, in water and 1.9 and 2.0 on water (Table 5; integration from −12 to −3.5 also given). While the number of solute−solvent interactions is similar at the ground and transition states, the associated energies for those interactions are stronger at the transition structure (Figure 4). Destabilization of the reactant on water, in addition to increased solute−solvent interactions at the transition structure, was found for the R = OCH_3 and Br substituted ethers with the number of waters interacting with the reactant decreasing to 1.0 and 1.4, respectively, compared to 1.9 for CH_3. The increase in solute−solvent interactions from the reactant to activated complex is also larger for the on water environment compared to the in water one, particularly for allyl naphthyl ether, which increases by about one water molecule (Table 5). The results suggest that while enhanced hydrogen-bonding interactions at the transition state is the primary contributor toward a reduction in the activation barrier, destabilization of the reactant plays a large role for the on water systems. The hydrogen bonds become stronger for the transition state owing to the enhanced charges at the reacting oxygen of the Claisen rearrangements (Table 6). The overall results support the fact that hydrogen bonding is very sensitive to charge distributions,[53] so it is more affected by the progression from the reactant to the activated complex in water than the weaker dipole−dipole interactions in the less polar solvents.

Radial Distribution Functions. The solute−solvent structure for the Claisen rearrangements in water and on water can be further characterized by radial distribution functions, $g(R)$. Hydrogen bonding between the reacting oxygen of the allyl *p*-R-phenyl ethers and the hydrogen of water, O(ether)−H(water), should yield contacts shorter than 2.7 Å. The corresponding

(53) (a) Blake, J. F.; Lim, D.; Jorgensen, W. L. *J. Org. Chem.* **1994**, *59*, 803–805. (b) Blake, J. F.; Jorgensen, W. L. *J. Am. Chem. Soc.* **1991**, *113*, 7430–7432.

Table 6. Charges for the Claisen Rearrangement Transition Structure (and Reactant in Parentheses) of Allyl *p*-R-phenyl Ether[a]

R	O1	C2	C4	C5
		In Water		
OCH_3	−0.368 (−0.256)	−0.089 (−0.045)	−0.224 (−0.338)	−0.135 (−0.173)
CH_3	−0.385 (−0.267)	−0.087 (−0.027)	−0.178 (−0.346)	−0.222 (−0.193)
Br	−0.402 (−0.248)	−0.099 (−0.061)	−0.149 (−0.332)	−0.243 (−0.214)
		On Water		
OCH_3	−0.380 (−0.256)	−0.100 (−0.082)	−0.186 (−0.316)	−0.169 (−0.257)
CH_3	−0.383 (−0.255)	−0.064 (−0.058)	−0.165 (−0.341)	−0.248 (−0.199)
Br	−0.389 (−0.249)	−0.124 (−0.042)	−0.118 (−0.332)	−0.275 (−0.220)

[a] CM3 charges scaled by 1.14 from QM/MM/MC simulations. Atom numbering scheme is given in Figure 1.

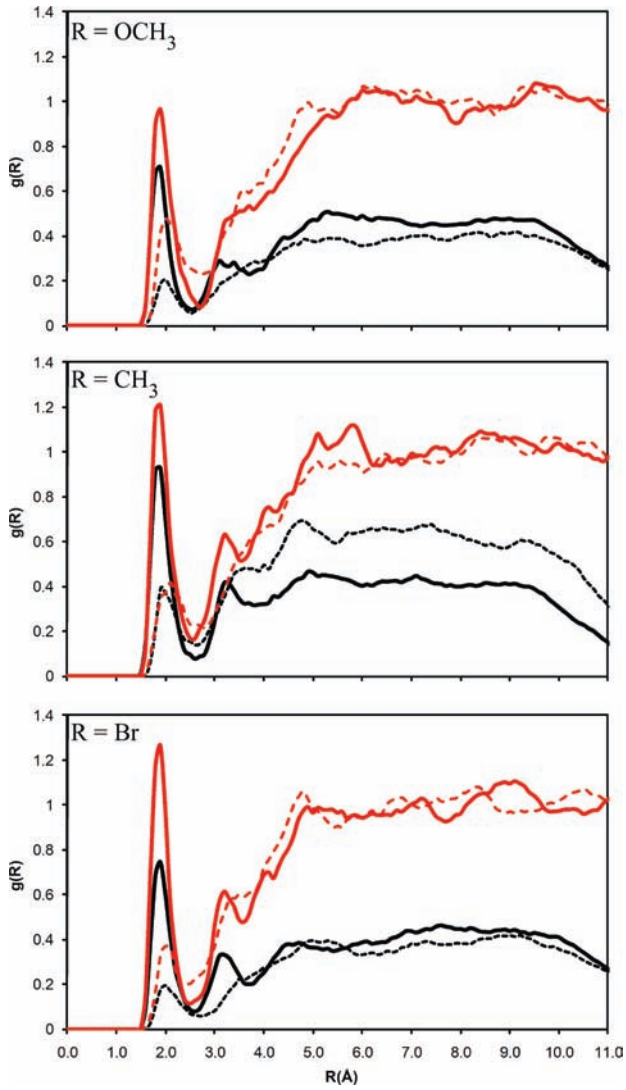

Figure 5. Computed O(ether)−H(water) radial distribution function for the Claisen rearrangement reactions of allyl *p*-R-phenyl ethers: in water transition structure (solid red), in water reactant (dashed red), on water transition structure (solid black), and on water reactant (dashed black) at 25 °C.

$g_{OH}(R)$ gives the probability of finding a hydrogen of a water at a distance R from the reacting oxygen of the ether. Accordingly, both the in water and on water, rearrangement reactions show a well-defined first peak centered around 1.9 Å with a minimum around 2.5−2.7 Å that reflects the hydrogen bonds (Figure 5). In both cases, the hydrogen bonding is clearly greatest for the activated complex in all three substituents; however, the in water transition structure shows a larger number of O(ether)−H(water) interactions with the homogeneous water molecules (red solid line in Figure 5) compared to the interfacial water interactions for the on water transition structure (solid black line). Integration of the peaks from 0 to 2.5−2.7 Å confirm a reduced number of site-specific O(ether)−H(water) hydrogen bonds for the allyl *p*-R-phenyl ether transition structures on water when compared to the in water environment, i.e., 1.3 from 1.7 for R = OCH_3, 1.9 from 2.0 for R = CH_3, and 1.6 from 1.8 for R = Br (Table 7).

Table 7. Number of Water Molecules Interacting with the Reacting Oxygen of Allyl *p*-R-phenyl Ethers and Allyl Naphthyl Ether for the Claisen Rearrangement Reactant (GS) and Transition Structure (TS) in Water and on Water from Radial Distribution Functions[a]

	in water		on water	
R	GS	TS	GS	TS
OCH_3	1.4	1.7	0.5	1.3
CH_3	1.2	2.0	1.1	1.9
Br	0.8	1.8	0.6	1.6
naphthyl	1.0	1.3	0.9	1.5

[a] Integration of the first peak of Figures 5 and S7 (Supporting Information) to 2.5−2.7 Å.

The resultant destabilization of the transition structure on water correlates well with the predicted reduction in rates compared to the homogeneous aqueous conditions. Inspection of the orientations of the solutes at the interface found the aromatic ring to lie flat on the water surface with a tilt toward the reacting oxygen throughout the reaction pathway when hydrophobic substituents, i.e., CH_3 and Br, were included on the ring. Site-specific interactions between the hydrophobic and hydrophilic substituents and the interfacial waters are predicted to act as an "anchor" for the molecules at the oil/water interface, dictating their overall accessibility to the surface water. The more hydrophilic the substituent, the larger the tilt toward the substituent group on the water surface and, as a result, the larger the tilt away from the reacting oxygen (similar to a "see-saw" motion). The computed geometry orientations, radial distribution functions, and solute−solvent energy pair distributions all predict a greater loss of hydrogen bonds for the hydrophilic OCH_3 substituted rearrangement reaction on water compared to the hydrophobic CH_3 and Br groups. These results are consistent with recent experimental tilt-angle measurements of coumarins at the air/water interface using electronic sum frequency generation (ESFG) spectroscopy; the most hydrophobic coumarins were reported to experience an intermediate polar environment, whereas moderately water-soluble ones felt the most nonpolar environment.[54]

The interactions between O(ether) and H(water) in the reactant were also reduced for the on water reactions compared to in water; however, the loss was more dramatic for the OCH_3-

(54) Sen, S.; Yamaguchi, S.; Tahara, T. *Angew. Chem., Int. Ed.* **2009**, *48*, 6439–6442.

phenyl system compared to the more hydrophobic substituents. For example, integrating the first peak to 2.6−2.7 Å for the R = OCH_3 reactant yields 1.4 and 0.7 hydrogen bonds in water compared to on water, respectively, while the number for R = CH_3 remains relatively constant at 1.2 and 1.1 (Table 7). Despite a loss in favorable site-specific hydrogen bonds for the more hydrophilic ether, the strong electron-donating ability of OCH_3 relative to CH_3 provides an intramolecular stabilization at the transition state that is able to offset the loss of hydrogen bonding and provide an overall faster rate of reaction.

Hydrophobic Effects. To focus on the role hydrophobic effects play in the rate acceleration of aromatic Claisen rearrangements, the variation of the solute's solvent accessible surface area (SASA) at the ground and transition state was examined. The same pattern is observed for the allyl *p*-R-phenyl ethers and allyl naphthyl ether: the reactant has a SASA which has a larger exposed surface than the activated complex by ca. 20−25 Å^2. It is known that the change in SASA and free energy of hydration for hydrocarbon systems show a linear correlation with a proportionality constant of about 0.01 kcal/mol/Å^2.[42,55] This suggests that the hydrophobic effect should not contribute more than 0.5 kcal/mol to the reduced free energies of activation for these rearrangements in water. The results are consistent with early AM1-SM2 calculations by Cramer and Truhlar on allyl vinyl ether (and derivatives) that predicted the accelerative hydrophobic effect to be small and not sensitive to structure.[14] Solutes utilizing the on water environment benefit less from the hydrophobic effect, as the allyl hydrocarbon portion was found to minimize the interaction with water by occupying almost exclusively the gas-phase portion of the air/water interface. The ethers with hydrophilic substituents on the phenyl ring were particularly affected, as the radial distribution calculations found a reduced number of water interactions with the allyl chain.

Continuum Solvent Models. The polarizable continuum model (PCM) presents an alternative method for exploring solvent effects.[36] However, ab initio and DFT calculations coupled to continuum solvent models have been consistently unsuccessful in predicting rate differences between protic and aprotic solvents for a large variety of organic reaction types.[22] For example, previous calculations on allyl *p*-tolyl ether using B3LYP/6-31G(d) and the integral equation formalism variant of PCM (IEFPCM) failed to predict the accurate sequence of reaction rates in five different solvents.[44] However, multiple improvements to the PCM framework[56] have been subsequently implemented into the newly released Gaussian 09 software to enhance accuracy.[34] For example, IEFPCM now uses Karplus and York's conductor screening model for building the solute's cavity and computing the reaction field.[57] In the light of the implication of solvent on rates, the new IEFPCM methodology has been tested in this work in conjunction with B3LYP/6-311+G(2d,p) to optimize transition structures and ground states for the allyl *p*-R-phenyl ether and allyl naphthyl ether rearrangements (Tables 4, 8 and 9). Geometries for the stationary points on the free-energy profiles were initially located in vacuum at the CBS-QB3 and B3LYP/6-311+G(2d,p) theory levels. The gas-phase free-energy activation barriers were found to be in reasonable agreement with experimentally measured values (Table 8). For example, $\Delta G^{\ddagger}$ values of 35.1 and 34.5 kcal/mol for the allyl *p*-tolyl ether rearrangement using CB3-QB3 and B3LYP/6-311+G(2d,p), respectively, were in good agreement with the experimentally reported value of 38.5 kcal/mol.[15] The PDDG/PM3 method systematically overestimated the gas-phase results in a similar magnitude compared to the solution-phase calculations (Tables 2 and 8).

Table 8. Gas-Phase Activation Barriers, $\Delta G^{\ddagger}$ (kcal/mol), at 25 °C for the Claisen Rearrangement of Allyl *p*-R-phenyl Ethers (R = OCH_3, CH_3, and Br)

	$\Delta G^{\ddagger}$		
	OCH_3	CH_3[a]	Br
CBS-QB3	35.1	35.1	35.1
B3LYP/6-311+G(2d,p)	34.0	34.5	34.4
PDDG/PM3	51.3	50.7	51.2

[a] Gas-phase $\Delta G^{\ddagger}$(exptl) = 38.5 kcal/mol at 170 °C (ref 15).

Table 9. Free Energy of Activation, $\Delta G^{\ddagger}$ (kcal/mol), at 25 °C for the Claisen Rearrangement of Allyl *p*-R-phenyl Ethers in Solution using B3LYP/6-311+G(2d,p)/PCM

R	water (calcd)	water (exptl)[a,b]	*n*-pentadecane (calcd)	*n*-tetradecane (exptl)[a]
OCH_3	31.9	33.5	33.1	36.4
CH_3	32.3	34.4	33.7	37.4
Br	32.1	34.9	33.6	37.7

[a] 170 °C (ref 17). [b] 28.5% EtOH−H_2O.

Geometry optimizations at the B3LYP/6-311+G(2d,p)/PCM level were then executed in five different solvents for the allyl naphthyl ether (Table 4) and in water and *n*-pentadecane for the allyl *p*-R-phenyl ether rearrangements (Table 9). The DFT/PCM model was unsuccessful in reproducing the observed changes in the rate of reaction. For example, the allyl naphthyl ether reaction was predicted to have essentially identical activation barriers, $\Delta G^{\ddagger}$ of ca. 20 kcal/mol, in water, methanol, acetonitrile, and DMF (Table 4), contrary to the experimentally reported differences in rates.[7] Specific changes in hydrogen bonding are expected to be important along the reaction path, but they are not explicitly treated in the continuum model. The QM/MM/MC calculations clearly overcome this limitation (Tables 2−4). Ideally, the use of B3LYP/6-311+G(2d,p) or higher theory levels coupled to the current QM/MM approach could provide reasonable quantitative accuracy for absolute activation barriers while correctly reproducing the solvent effects. Unfortunately, the use of DFT methods in the QM/MM framework is impractical in view of the need for thorough configurational sampling in the fluid simulations, i.e., 120 million QM single point energy evaluations per Claisen rearrangement free-energy map. An ab initio QM/MM approach that includes the solvent reaction coordinate, such as Gao's modern valence bond theory (MOVB) method[58] or Warshel's empirical valence bond (EVB) treatment,[59] may provide an alternative approach for computing on water reactions. Either method would be an interesting avenue to pursue in future studies in order to assess any potential solvent fluctuation differences between the in water and on water environments.

Conclusions

In summary, QM/MM/MC simulations have been carried out for the Claisen rearrangements of allyl *p*-R-phenyl ether, where

(55) Eisenberg, D.; McLachlan, A. D. *Nature* **1986**, *319*, 199–203.
(56) (a) Improta, R.; Barone, V.; Scalmani, G.; Frisch, M. J. *J. Chem. Phys.* **2006**, *125*, 054103:1−9. (b) Improta, R.; Scalmani, G.; Frisch, M. J.; Barone, V. *J. Chem. Phys.* **2007**, *127*, 074504:1−9.
(57) York, D. M.; Karplus, M. *J. Phys. Chem. A* **1999**, *103*, 11060–11079.
(58) Mo, Y.; Gao, J. *J. Phys. Chem. A* **2000**, *104*, 3012–3020.
(59) Aqvist, J.; Warshel, A. *Chem. Rev.* **1993**, *93*, 2523–2544.

R = OCH_3, CH_3, and Br, and allyl naphthyl ether on water, in water, and in 14 additional solvents yielding good accord between the computed and observed variations in the free energies of activation. Rate accelerations for the Claisen rearrangements are shown to be correlated to increasing solvent polarity and in the case of the on water environment are derived from the ability of the interfacial waters to stabilize the transition state. Destabilization of the reactant also played a large role for the on water systems. An orientation analysis of multiple snapshots of the reacting solute relative to the surface of the slab (perpendicular to the *z*-axis) found that the aromatic ring tended to lie essentially flat on the surface with a slight tilt toward the oxygen when hydrophobic substituents, i.e., CH_3 and Br, were included on the ring. The inclusion of hydrophilic substituents, i.e. OCH_3, on the ring tilted the reacting oxygen away from the interfacial waters and toward the substituent. Radial distribution functions and solute−solvent energy pair distributions confirm a reduction in the site-specific hydrogen-bonding interactions with the surface waters as the aromatic ethers became more hydrophilic. These results are consistent with recent experimental tilt-angle measurements of coumarins at the air/water interface; the most hydrophobic coumarins were reported to experience an intermediate polar environment, whereas moderately water-soluble ones felt the most nonpolar environment.[54] Hydrophobic effects, where the solvent accessible surface area decreases in going from ground to transition state, were determined to contribute no more than 0.5 kcal/mol toward lowering the activation barrier in a homogeneous aqueous environment and were substantially diminished on water, as much of the reacting allyl chain favored occupying the organic phase. Solvent polarizability was not found to provide a substantial contribution on the rates or geometry of the reaction. High-level ab initio and density functional theory (DFT) calculations at the CBS-QB3 and B3LYP/6-311+G(2d,p) theory levels, respectively, coupled to the polarizable continuum model (PCM) were carried out, but they did not predict the correct sequence of reaction rates in solution.

Overall, the on water reactions benefited most from site-specific hydrogen bonding between the interfacial waters and the transition structure. The addition of hydrophobic substituents increased the polarity felt by the solute at the air/water interface, which provided a superior environment for enhanced rate accelerations. Such information could possibly be exploited in the preparation of organic molecules via a safer and more environmentally friendly on water environment.

Acknowledgment. Gratitude is expressed to Prof. W. L. Jorgensen for the additions to the BOSS program that allow performance of on water calculations. We gratefully acknowledge support of this research from Auburn University and the Alabama Supercomputer Center. Discussions with Prof. Peter Livant are also appreciated.

Supporting Information Available: OPLS atom types for solvents; computed and experimental densities and ΔH_{vap} for solvents; additional illustrations of on water allyl *p*-tolyl ether and allyl naphthyl ether transition states; additional geometries and charges for Claisen rearrangements; additional solute−solvent energy pair distributions; energies, frequencies, and coordinates of all structures computed using ab initio and DFT methods; and complete ref 34. This material is available free of charge via the Internet at http://pubs.acs.org.

JA908680C